

An Ag-Dependent Approach Based on Adaptive Mechanisms for Investigating the Regulation of the Memory B Cell Reservoir

Alexandre de Castro

Laboratory of Computational Mathematics, National Center of Technological Research on Informatics for Agriculture (Embrapa Agriculture Informatics), Brazilian Agricultural Research Corporation (Embrapa), Campinas, Brazil

1. Introduction

Twenty years ago, Farmer, Packard, and Perelson presented an elegant dynamical model [1] to study Idiotypic Network theory [2-19], in which they showed that every molecular and cellular binding site (cell receptor) can be modeled by binary *bit-strings* of length ℓ . In such a model, an antibody molecule can always recognize an antigen when there is complementarity between their *bit-strings*. The coincidence of antigens and lymphocyte receptors (lock-and-key model) is determined by considering the number of complementary bits [8,20]. For instance, if a B lymphocyte is represented by a binary string 00010101 ($\ell = 8$) and an antigen is represented by the 11101010 binary string, the immune response is activated (Fig. 1). The match between bit-strings does not need to be perfect, however; some bit positions are allowed in which two strings differ. These differences between strings (mismatches) reflect the degree of affinity between the entities of the immune system in mammals and determine the quality of the response.

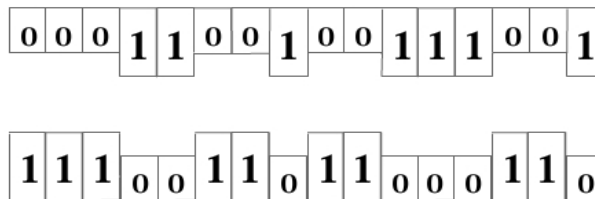


Fig. 1. Pictorial representation of the binding site (cell antigen) by means of a bit-string frame [6].

In another work, Lagreca *et al.* (2001) [21] also proposed a dynamic model that was based on the recognition of shapes or patterns using bit-strings, but used the iterative solution of a coupled map system that enabled the treatment of high dimensions. In the model created by

Lagreca *et al.* (2001), the B cell and the antibody populations are treated as a clone pools because their receptors are represented by the same bit-strings. Because a bit-string can be considered as the binary representation of an integer, the model indexes each clone to an entire σ , and the temporal evolution of the populations is described by the $N(\sigma, t)$ concentration. The model also considers a source term that simulates the role played by the bone marrow, where new bit-strings are presented. The death or depletion of clones occurs in two ways: 1) by means of natural death (apoptosis), described by the parameter d ; and 2) by means of a general suppression mechanism, described by a Verhulst-like factor [22]. This factor is widely used in simulations of biological systems, because it limits the maximum population that can survive in a particular environment [22]. The Lagreca *et al.* model (2001) considers this maximum B cell population (N_{\max}) to be the same for every clone, and the populations are normalized by the $y(\sigma, t) = N(\sigma, t) / N_{\max}$ function.

Thus, considering a discrete temporal evolution, the following coupled map set proposed by Lagreca *et al.* [21] allows part of an adaptive immunological system to be simulated:

$$y(\sigma, t+1) = (1 - y(\sigma, t)).$$

$$\left\{ m + (1-d)y(\sigma, t) + b \frac{y(\sigma, t)}{y_{tot}(t)} \left[(1 - a_h)(y(\bar{\sigma}, t) + y_F(\bar{\sigma}, t)) + a_h \sum_{i=1}^B (y(\bar{\sigma}_i, t) + y_F(\bar{\sigma}_i, t)) \right] \right\}, \quad (1)$$

where $(1 - y(\sigma, t))$ is the Verhulst-like factor; $y_F(\sigma, t)$ describes the antigen population, characterized by a σ bit-string which, in this case, represents distinct antigenic determinants; $\bar{\sigma}$ represents the perfect complementary shape of σ ; and $\bar{\sigma}_i$ are the nearest neighbors of $\bar{\sigma}$ in a B -dimensional hypercube. The term m represents the population of cells produced by bone marrow; the $(1-d)$ term represents the percentage of the lymphocyte population that survives a natural cell death (apoptosis); and the other terms describe the clonal proliferation $y(\sigma, t)$ that occurs because of interaction with complementary B cells and/or antigens.

The b parameter is a clonal proliferation constant (typically related to the mean number of new cells produced by the pre-existing cells), and $y_{Tot}(t)$ is the total population, given by equation 2:

$$y_{tot}(t) = \sum_{\sigma} [y(\sigma, t) + y_F(\sigma, t)] \quad (2)$$

The parameter a_h is the connectivity factor between a specific *bit-string* and the specular image of its neighbors. When $a_h = 0.0$, only a perfect coincidence of complementary shapes is valid. When $a_h = 0.5$, a bit-string can recognize equally both its own specular image and the nearest neighbors of its specular image. The temporal evolution of the antigen pool is defined by equation 3.

$$y_F(\sigma, t+1) = y_F(\sigma, t) - k \frac{y_F(\sigma, t)}{y_{tot}(t)} \left\{ (1 - a_h)y(\bar{\sigma}, t) + a_h \sum_{i=1}^B y(\bar{\sigma}_i, t) \right\}, \quad (3)$$

where k is an antigen removal parameter that represents the interactions with the clonal populations.

In fact, it is well-known that the soluble antibody population is one of the essential mechanisms of immunological response regulation [23-25]. However, despite the pioneering work of Lagreca *et al.* (2001) in developing a coupled map for studying the behavior of the mammalian immune system, their model did not consider these populations [1-6], which makes the model incomplete with respect to the regulation of the immune response by adaptive mechanisms. This omission opens up the possibility of extending their work by taking the soluble antibody populations into account. We have performed that work and present our immunological modeling and simulation findings in this paper.

2. Materials and methods

In this section, we briefly describe the Verhulst approach and provide details of an extension to the Lagreca *et al.* (2001) model, which includes an antibody variable to address the regulation of the structural mechanisms that are mediated by the immunoglobulin population. This variable was not considered in the simplified model proposed by Lagreca *et al.* [21].

2.1 The Verhulst approach

Since the early nineteenth century, studies on population dynamics have been developed to identify possible nonlinear behaviors. One of the first efforts aimed at predicting biological population behavior was made by Pierre François Verhulst (1804-1849), a Belgian mathematician. He proposed a nonlinear model in which the death rate was proportional to the square of the number of individuals in the population. The model can be expressed by differential equations [26-30], as follows:

$$\frac{dN}{dt} = AN - BN^2$$

where N is the number of individuals, and A and B are constants related to the growth rate and the population growth limitation, respectively.

The Verhulst model was used again in 1976, by Robert May [27], to study insect population dynamics. In his experiments, he replaced the original differential method by what is now known as the *map* methodology, in which each value is obtained by its anterior value:

$$N_1 = AN_0 - BN_0^2$$

$$N_2 = AN_1 - BN_1^2$$

$$N_{n+1} = AN_n - BN_n^2$$

At the limit of saturation, $AN_{max} - BN_{max}^2 = 0$, then $N_{max} = 0$ or $N_{max} = A/B$.

Solving $\frac{N_{n+1}}{N_{max}} = A \frac{N_n}{N_{max}} - B \frac{N_n^2}{N_{max}} \frac{N_{max}}{N_{max}}$ and inserting $x_n = \frac{N_n}{N_{max}}$ results in the following:

$x_{n+1} = Ax_n - Bx_n^2$. Defining the parameter A (birth rate) = r (control parameter), we obtain:

$$x_{n+1} = rx_n(1 - x_n), \quad x_n \in [0, 1] \quad (4)$$

In equation (4), known as a *logistic map*, the values for $x_n \in [0, 1]$ and r are dimensionless and represent population fractions as a function of each of the n iterations, respectively, while r is a constant that represents the population growth rate in each new iteration. The term $(1 - x_n)$ is known as the Verhulst factor [21,31,32].

The bifurcation diagram of the logistic map is built by the iterative resolution of the logistic equation, starting with an arbitrary x_0 initial value and choosing sequential values for the parameters r , $r \in [r_{min}, r_{max}]$. The bifurcation diagram of the logistic equation is shown in Fig. 2.

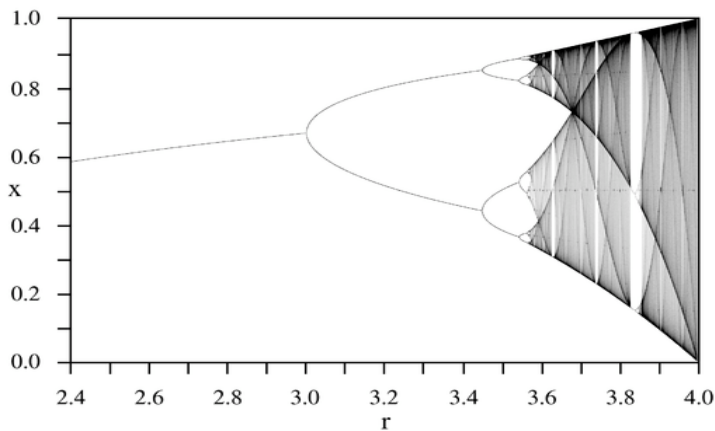


Fig. 2. Classical bifurcation diagram of a logistic map as a function of the parameter r [33].

In Fig. 2, the attractor is a fixed point up to the first bifurcation. For each bifurcation, there occurs a period of duplication before the system reaches the chaotic phase. However, to illustrate the dynamics of this simple model, it is important to show that, for r between 0 and 1, the population death rate is not dependent on the initial population. With r between 1 and 3, the population is prone to an attractor of a fixed point type. For r greater than 3.54, the population wiggles between values of 8, 16, 32, and so on. At approximately $r=3.57$, the end of the cascade duplication period occurs and chaos begins. From this value, small variations in the initial population produce very different results over time, which is the fundamental characteristic of chaos. For r greater than 4, the populations are outside the $[0, 1]$ interval.

It is possible to demonstrate that the Lagreca *et al.* (2001) model for clonal populations reduces to equation 4 when there is no further exposure of the system to the antigens. This reduction occurs because, under this one condition, the additive term (m) in equation 1, which represents the bone marrow contribution for the immune repertoire, is very small when compared with the clonal proliferation parameter (b) [34,35]. A detailed

demonstration of this assertion is presented in subsection 3 of the section on the model parameters.

2.2 Simulation model

As in the Lagreca *et al.* (2001) model [21], our extended Ag-dependent model has molecular receptors of B cells that are represented by bit-strings with 2^B of diversity, where B is the number of bits in the string. The individual components of the immune system represented in the extended model are B cells, antibodies, and antigens located at the vertices of hypercubes of size B. B cells (clones) are characterized by their surface receptors and are modeled by a binary bit-strings. The epitopes [1,8,17-19], which are portions of an antigen that can be connected by the B cell receptor (BCR), are also represented by bit-strings. The antibodies have receptors (paratopes) [1,8,17-19] that are represented by the same bit-string models as the BCR B cell that produced them. Thus, the new dynamic equations that describe the behavior of the adaptive immune system, taking into account the inclusion of antibody populations, are the following:

$$y(\sigma, t + 1) = (1 - y(\sigma, t)) \left\{ m + (1 - d) y(\sigma, t) + b \frac{y(\sigma, t)}{y_{tot}(t)} \zeta_{a_h}(\bar{\sigma}, t) \right\}, \quad (5)$$

for a clonal population, with complementary shapes included in the term $\zeta_{a_h}(\bar{\sigma}, t)$,

$$\zeta_{a_h}(\bar{\sigma}, t) = (1 - a_h)(y(\bar{\sigma}, t) + y_F(\bar{\sigma}, t) + y_A(\bar{\sigma}, t)) + a_h \sum_{i=1}^B (y(\bar{\sigma}_i, t) + y_F(\bar{\sigma}_i, t) + y_A(\bar{\sigma}_i, t)).$$

The clonal populations can range from the value generated by bone marrow (m) up to its maximum value (unity) because the Verhulst factor is a limiting factor [21,31,32].

In the model presented in this paper, the $y_{Tot(t)}$ term represents the sum of the components that belong to an adaptive subset of the immune system, as described in the introduction to this work. Such elements, when added to antibody populations, are expressed as bit-string concentrations.

Therefore, the sum of every adaptive component considered by our model is given by equation (6).

$$y_{tot}(t) = \sum_{\sigma} [y(\sigma, t) + y_F(\sigma, t) + y_A(\sigma, t)] \quad (6)$$

The temporal evolution of the antigens can be defined by equation (7).

$$y_F(\sigma, t + 1) = y_F(\sigma, t) - k \frac{y_F(\sigma, t)}{y_{tot}(t)} \left\{ (1 - a_h) [y(\bar{\sigma}, t) + y_A(\bar{\sigma}, t)] + a_h \sum_{i=1}^B [y(\bar{\sigma}_i, t) + y_A(\bar{\sigma}_i, t)] \right\}, \quad (7)$$

The antibody population is described by a group of 2^B variables, also defined by a B-dimensional hypercube, interacting with the antigen populations of equation (8).

$$y_A(\sigma, t+1) = y_A(\sigma, t) + b_A \frac{y(\sigma, t)}{y_{tot}(t)} \left[(1 - a_n) y_F(\bar{\sigma}, t) + a_n \sum_{i=1}^B y_F(\bar{\sigma}_i, t) \right] - k \frac{y_A(\sigma, t)}{y_{tot}(t)} \zeta_{a_n}(\bar{\sigma}, t), \quad (8)$$

where b_A is the antibody proliferation parameter; and k is the parameter related to the antibodies and antigens that will be removed.

In our model, equation 8, which considers the adaptive interactions that have been described in the specialized literature, is included. Thus, antibody proliferation is given by the recognition $y_A(\sigma, t) \Leftrightarrow y_F(\bar{\sigma}, t)$ [1,8,17-19]. The antibody population is regulated by the intersection of $y_A(\sigma, t) \Leftrightarrow y(\sigma, t)$ [1,8,17-19], $y_A(\sigma, t) \Leftrightarrow y_F(\bar{\sigma}, t)$ [1,8,17-19], and $y_A(\sigma, t) \Leftrightarrow y_A(\bar{\sigma}, t)$ [19,36]. In all cases, the connectivity between the first two neighbors was

considered. The factors $\frac{y_F(\sigma, t)}{y_{TOT}(t)}$ and $\frac{y_A(\sigma, t)}{y_{TOT}(t)}$ also help to regulate the antigen and antibody populations, while the term $\frac{y(\sigma, t)}{y_{TOT}(t)}$ is the corresponding clonal regulation factor involved in the formation of immunological memory.

The role performed by the clonal regulation factor, in addition to helping with the B cell response regulation, is fundamental to the regulation of the memorization ability and clonal homeostasis [37-39]. The importance of the effect of the clonal regulation factor over immune system memory evolution is shown in Fig. 3. Three distinct situations are possible:

1. antibody populations are included in the model (which corresponds to the model proposed in this work);
2. antibody populations are not included in the model (which corresponds to the Lagreca *et al.* [21] model);
3. memory expansion is not limited by the clonal regulation factor (which corresponds to the results obtained by P. G. Etchegoin [40]).

Fig. 3 illustrates the situation in which growth capacity increases indefinitely, which is when the clonal regulation factor is suppressed in the modeling phase. This shows that clonal regulation can be fundamental to the immune system reaching clonal homeostasis.

In the proposed Ag-dependent model, each bit-string is associated with an integer that is situated in an interval, $0 \leq M \leq 2^B - 1$, and each represents a clonal population, antigen, or antibody located in the B-dimensional hypercube vertex. The neighbors i of a specific σ or $\bar{\sigma}$ are expressed by the Boolean functions $\sigma_i = (2^i - 1 \text{ xor } \sigma)$ or $\bar{\sigma}_i = (2^i - 1 \text{ xor } \bar{\sigma})$, respectively. The complementary way of obtaining σ is obtained by $\bar{\sigma} = M - \sigma$ [21].

An example of the way in which the B cell, antibody, or antigen populations are localized in 3-dimensional space is shown in Fig. 4.

For the cubic configuration in Fig. 4, the following algorithm describes how to obtain the first neighbors and the complementary shape of the B cell population identified by the integer $\sigma = 4$:

- For a cubic configuration ($B=3$), there exists a repertoire containing $2^B = 8$ integer numbers arranged in the cube vertex. These integer numbers represent the 8 different B cell populations;

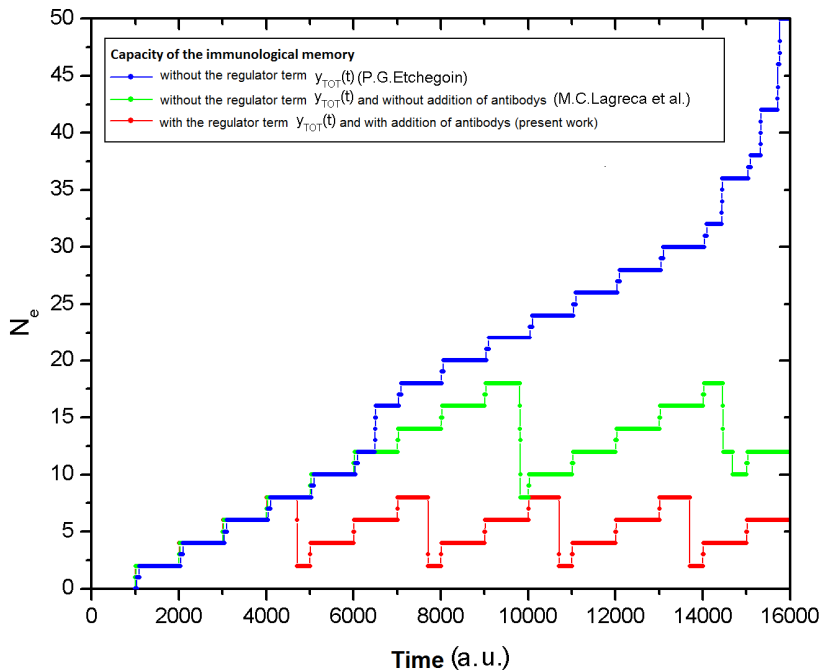


Fig. 3. Capacity of immune system memory in three distinct situations.

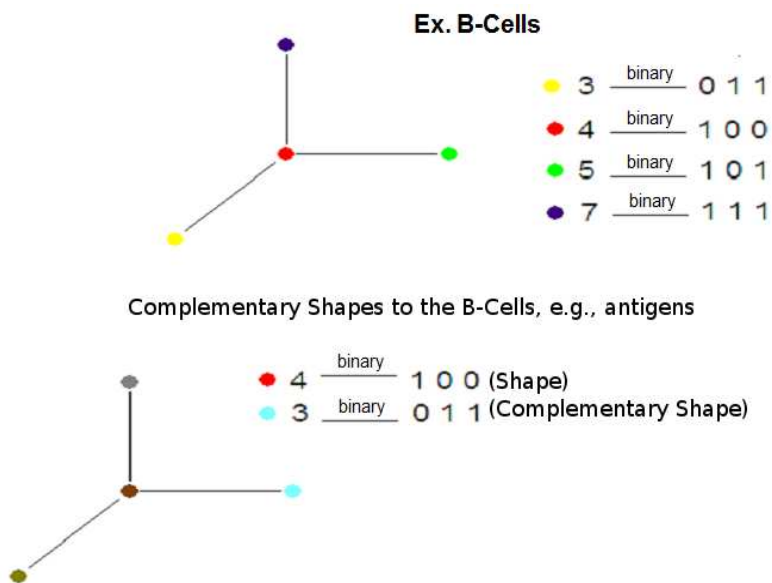


Fig. 4. Spatial arrangement of a B cell population that is identified by 4 integers. Antigens and antibodies also are spatially arranged in the same way, in various cubes.

- Each integer number M must be restrained in the interval $0 \leq M \leq 2^B - 1$; thus, each cube vertex is identified [16];
- With this condition, the smallest value of M is equal to 0 and the largest value is equal to 7. Consequently, the shape space S is equal to $\{0,1,2,3,4,5,6,7\}$;
- To represent the reactions of the lock-and-key type described in the introduction, every cell population in a cubic configuration needs to be represented by 8 bit-strings;

$$\sigma = 4 = \sum_{i=0}^2 2^i a_i = 2^0 a_0 + 2^1 a_1 + 2^2 a_2 = 4$$

If, for example, $a_2 = 1$, $a_1 = 0$ and $a_0 = 0$, then in this case 4 in the decimal base corresponds to (1 0 0) in the binary base;

- For the other 7 vertices of the cube:

$$\sigma = 0 = (000),$$

$$\sigma = 1 = (001),$$

$$\sigma = 2 = (010),$$

$$\sigma = 3 = (011),$$

$$\sigma = 4 = (100),$$

⋮

$$\sigma = 7 = (111);$$

- For a lock-and-key reaction to occur, there must be another shape $\bar{\sigma}$ that is complementary to $\sigma = 4$, i.e., $\bar{\sigma} = M - \sigma$ [16,21]. Then, $M = 2^B - 1 = 7$ and $\sigma = 4 \rightarrow \bar{\sigma} = M - \sigma = 7 - 4 = 3$, or (0 1 1), in a binary base. This complementary shape is, in principle, an antigen population. However, based on Immune Network Theory, B cells also recognize antibodies and other complementary lymphocytes [1,8,17-19,36];
- Last, search for the first neighbors of the complementary shape $\bar{\sigma} = 3$. If $\sigma_i = (2^i - 1 \text{ xor } \sigma)$ [16,21], then, for $B = 3$ ($i = 1,2,3$), we get the following:

$$\sigma_1 = (2^1 - 1 \text{ xor } 3) = 2(010),$$

$$\sigma_2 = (2^2 - 1 \text{ xor } 3) = 0(000),$$

$$\sigma_3 = (2^3 - 1 \text{ xor } 3) = 4(100).$$

In this example, a B cell population identified by $\sigma = 4$ or (1 0 0) would have recognized an antigen population that is perfectly complementary and is identified by $\bar{\sigma} = 3$ (0 1 1). The antigen populations identified as the first neighbors for $\bar{\sigma} = 3$ are 0, 2, and 4 and can be recognized by the $\sigma = 4$ B cell population, depending on the value of the connectivity parameter a_i , which is included both in our proposed model and in the Lagreca *et al.* model [21].

Also, for better visualization, we used a 3-dimensional spatial configuration. Similar constructions for this work were made for B -dimensional spaces. Therefore, equations (5) to (8) constitute a set of maps that describes the main interactions of the immune system between the entities that interact through the lock-and-key type of connection, in other words, adaptive immune system entities that self-recognize. Such an equation set is iteratively resolved, considering various initial conditions.

2.3 Simulation dynamics

In this section, we present the dynamics of the simulations that were used to reproduce the proposed experiments *in silico*, and we evaluate the behavior of the proposed model.

To simulate the behavior of the immune system by means of the proposed mathematical model, we developed computational applications in the Fortran programming language (IBM's Mathematical FORMula TRANslation System). The source code was compiled with GFortran (GNU Fortran Compiler) on a Linux Operating System platform. Simulations were performed by a 2 GHz processor, with 4 GB of random-access memory (RAM).

To establish the relationship between antigen mutation and the memory of the lymphocyte population, we performed 3 *in silico* experiments with 30 samples $E_{j,k} = E(j=1, \beta)(k=1, \gamma)$.

The same parameters were used in every $E_j = E(j=1, \beta)$ experiment to represent identical individuals. The antigens were identified by the following expression: $V_i E_{j,k} = V(i=1, \alpha)E(j=1, \beta)(k=1, \gamma)$, where the i , j , and k indexes describe the inoculation order, the experiment, and the sample, respectively. The number α is the number of inoculations in each experiment, β is the number of experiments, and γ is the number of samples in each experiment.

The antigen injection simulations were performed every 1,000 temporal steps (in arbitrary units - a.u.), representing the administration of a new antigen dose in a hypothetical mammal. In the first experiment, we injected 110 different antigen populations in the sample, in the second, 250, and, in the third, 350. To represent the mutation within a population of the same antigen, we used 10 different seeds for the pseudo-random number generator. In the first experiment, a seed was associated with each sample, and the same set of seeds was used to perform the other experiments. In this way, to represent the mutation, we considered that inoculated antigens in the same position belonged to the same species and underwent a mutation for each different sample. The difference between the samples is in the bit-string variation of the inoculated antigens, and the difference between the experiments is in the duration of the time steps. The design of the experiments and the antigen identification used in this work are shown in Fig. 5.

In the schematic diagram shown in Fig. 5, the antigen (i.e., a virus strain) is identified as V1E12, which is the mutation of the antigen V1E11 (belonging to an antigen population of the same species), and the antigen V2E11 is different from the V1E11 antigen (which belongs to various antigen populations).

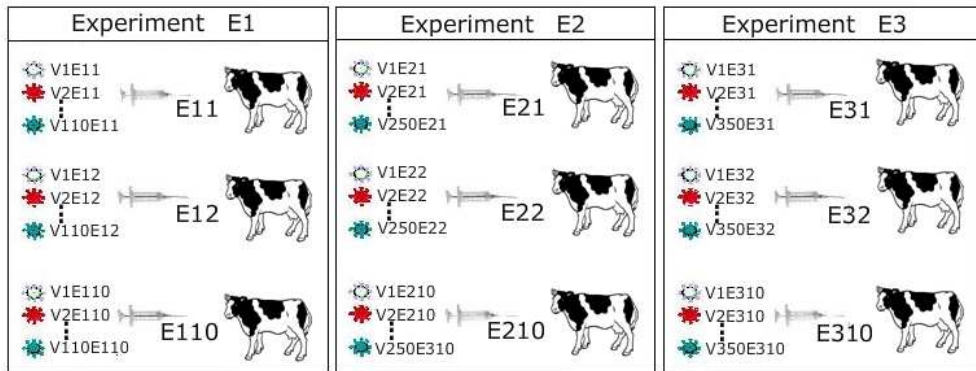


Fig. 5. In each experiment, different lifetimes were considered for individual hypothetical mammals. The lifetime (“lifespan”) for E1, E2, and E3 is 110000, 250000, and 350000 respectively.

2.4 Model parameters

The following table shows the ranges for the parameters used in our simulations, based on the literature.

| Symbol | Function | Value used in the model | Information obtained from the literature |
|----------|------------------------------------|--|---|
| <i>d</i> | Apoptosis | 0.99 | De Boer <i>et al.</i> [41] (2001): 0.95 Bueno <i>et al.</i> [42] (1999): 0.95 Lima <i>et al.</i> [43] (2007): $d > 0.95$ |
| <i>m</i> | Source term | 10^{-7} if $p < 0.1$ 0.0 if $p \geq 0.1$ | Lagreca <i>et al.</i> [21] (2001): 0.0005 von Laera <i>et al.</i> [34] (2005): 0.01 Monvel <i>et al.</i> [38] (1993): $m \approx 0.0$ |
| <i>b</i> | Clonal proliferation | 2.0 | De Boer <i>et al.</i> [41] (2001): 2.5-3.0 Utzny <i>et al.</i> [44] (2001): 2.0 von Laera <i>et al.</i> [34] (2005): 1.2 |
| <i>k</i> | Removal of antibodies and antigens | 0.1 | von Laera <i>et al.</i> [34] (2005): 0.01-0.1 |

Table 1. Parameters used in the proposed model.

2.4.1 The apoptosis clonal parameter (*d*)

In the extended model presented in this paper, *d* represents the fraction of cells that is subjected to natural death (apoptosis) or programmed death; thus, $s + d = 1$, where $s = 1 - d$

is the fraction of cells that avoids apoptosis. In the literature, the apoptosis of lymphocytes is typically assumed to occur in percentages not less than 95% [41,43]. For the simulations developed in this study, the natural death parameter was fixed at 0.99 (99%). To give an idea of the effect of varying this parameter, the performances of the model for two different apoptotic events and for the first inoculation antigen were compared (See Fig. 6).

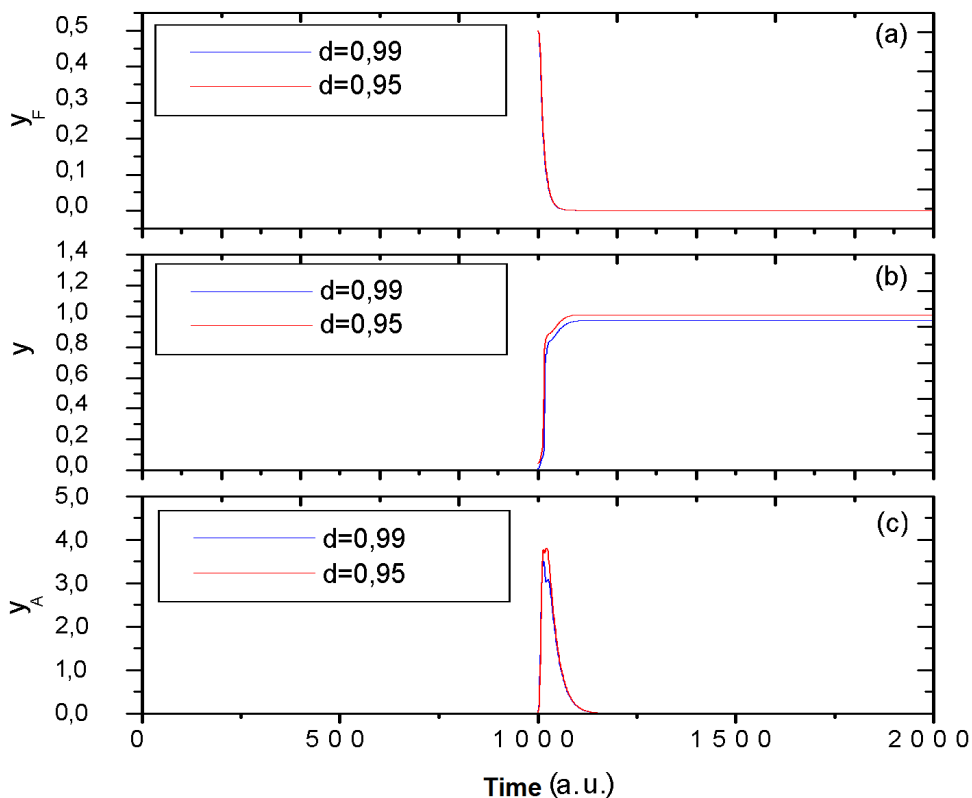


Fig. 6. Evolution of populations of antigens, B lymphocytes, and antibodies with respect to natural death parameter $d = 0.99$ and $d = 0.95$. The parameter $b_A = 100$ and initial antigen dosing $Ag_{inicial} = 0.5$. The virgin state of the system is the range of 0 to 1000.

2.4.2 The source term (m)

The source term m simulates the stochastic behavior of the bone marrow in the production of new lymphocytes [21,38].

In the model described in this work, if the pseudo-random number generator returns a value less than or equal to $p = 0.1$, the source term takes the value $m = 10^{-7}$, because m is experimentally small compared with the levels of lymphocytes produced in the immune response [34,35,38]. If the generator returns values greater than $p = 0.1$, the source term takes the value $m = 0.0$ [21].

2.4.3 The clonal proliferation parameter (b)

Both the pioneering work and the recent work in the literature on theoretical immunology present results on the dynamics of the immune system and the search for attractors of the fixed point type to determine *in machine* clonal homeostasis (equilibrium) in the virgin state (antigen without inoculation) and in the excited state (when an antigen is recognized by some clonal population) [37,38,40].

The condition $y_F = y_A = 0$ is satisfied when the virgin state of the immune system is considered, i.e., without the presentation of antigens, no antibodies are produced. Also, considering that the system only allows high-affinity connections (connections between perfectly complementary shapes), the connectivity factor $a_h = 0$.

In the virgin state, the sum total of the immune populations is restricted to B lymphocytes:

$$y_{Tot}(t) = \sum_{\sigma} [y(\sigma, t) + y_F(\sigma, t) + y_A(\sigma, t)] = \sum_{\sigma} y(\sigma, t)$$

Hence, equation 5 reduces to the following:

$$y(\sigma, t+1) = [1 - y(\sigma, t)] \{ m + (1-d)y(\sigma, t) + b \frac{y(\sigma, t)}{\sum_{\sigma} y(\sigma, t)} y(\bar{\sigma}, t) \}.$$

As in the dynamic simulation used in this work, the virgin state occurs in the interval of 0 to 1000 time steps, and only a pseudo-random number is drawn. Then,

$$\sum_{\sigma} y(\sigma, t) = y(\sigma, t) = y(\sigma^*, t) = y(t) = y_t \text{ and } y_t = y(\bar{\sigma}, t),$$

because, according to Immune Network Theory, for each lymphocyte population, there is another complementary population [17,18,19]. A more detailed explanation can be found in the results section.

Because the bone marrow term in the absence of infection (virgin state of the immune system) is much smaller than the clonal proliferation parameter ($m \ll b$) [34,35], we have the following:

$$y_{t+1} = [(1-d)y_t + by_t](1 - y_t) \text{ or } [1 - d + b]y_t(1 - y_t).$$

Defining $r \equiv 1 - d + b$, the equality results in the following: ($y_{t+1} = ry_t(1 - y_t)$, a logistic map-type equation). Moreover, for the system under study to evolve to a fixed point, the condition $1 < 1 - d + b < 3$ must be satisfied.

Consequently, taking into account an apoptosis parameter equal to $d = 0.99$, the clonal proliferation parameter b must be located within the following range: $1 < 1 + b - 0.99 < 3 \rightarrow 0.99 < b < 2.99$. In the simulations presented in this paper, the clonal proliferation parameter b was set to 2.0.

2.4.4 The antibody and antigen removal parameter (k)

The parameter for the removal of antigens and antibodies k was set to 0.1, to ensure that the populations of antigens and antibodies decay to zero before the antigen is presented.

This procedure, which is adopted for a new antigen, is applied only after the previous antigen has been completely removed [21.45].

2.4.5 Connectivity (a_h)

The connectivity parameter used was 7, so that 99% of the populations are coupled to their perfect complement, and only 1% of the populations are coupled to the first neighbors of their complement. The quality of the immune response is directly related to the degree of affinity among the elements of the adaptive system [8].

2.4.6 Bit-string length (B)

Considering the available hypercube immune populations represented by the model, the length of the bit-string B was set at 12. This value corresponds to $2^{12} = 4,096$ different antigens.

2.4.7 Antibody proliferation parameter (b_A)

In the model presented in this work, the initial antigenic dose ($Ag_{initial}$) was set to study the influence of parameter b_A on the immune memory in some simulations.

In other simulations, this parameter was set to study the consequences to the memory of varying the antigen dosage. To clarify, the limit value of $b_A = 0.0$ corresponds to the model previously proposed by Lagreca et al. [21], and the limit value of $Ag_{initial} = y_F = 0.0$ corresponds to the virgin state of the immune system.

3. Results

The clonal populations that were excited after selection by an antigen (or an antigen population) are shown in Fig. 7, as follows: (a) for the first antigen inoculation; and (b) for the second antigen inoculation, with a dosage of 0.1. In this evolution, two populations were excited with the first antigen inoculation at step 1000: the clonal population that recognized the specific antigen (B1 - Burnet idiotypic cells [18.19]) and the clonal population (J1 - Jerne anti-idiotypic cells [18.19]) complementary to B1. At step 2000, the second antigen was inoculated, and four populations survived: the clonal population that was selected by the second antigen (B2), the clonal population (J2) that is complementary to B2, the clonal population that was selected by the first antigen (B1), and the clonal population (J1) that is complementary to B1.

At step 1000, clonal populations B1 and J1 are excited when they are selected by the first antigen, as shown in Fig. 7 (a). However, in step 2000, when populations B2 and J2 are excited, the clonal populations B1 and J1 are already memories of the first antigen. To maintain the homeostasis of the system, there is a decrease in the concentrations of the four remaining populations, as shown in Fig. 7 (b).

3.1 Antigen persistence

The temporal evolution (kinetics) of the Burnet cells is shown in Fig. 8 for each antigen i . Fig. 8 shows that the population selected by the first antigen begins to decrease after the second inoculation.

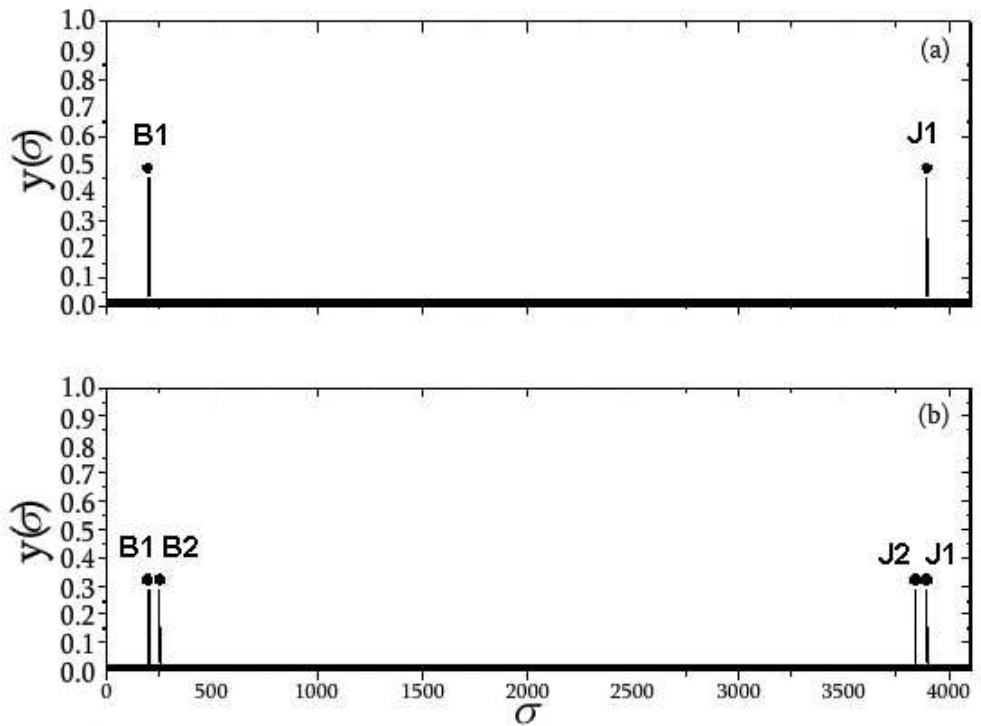


Fig. 7. Surviving clonal populations: (a) for the first antigen inoculated, and (b) for the first and second antigens inoculated.

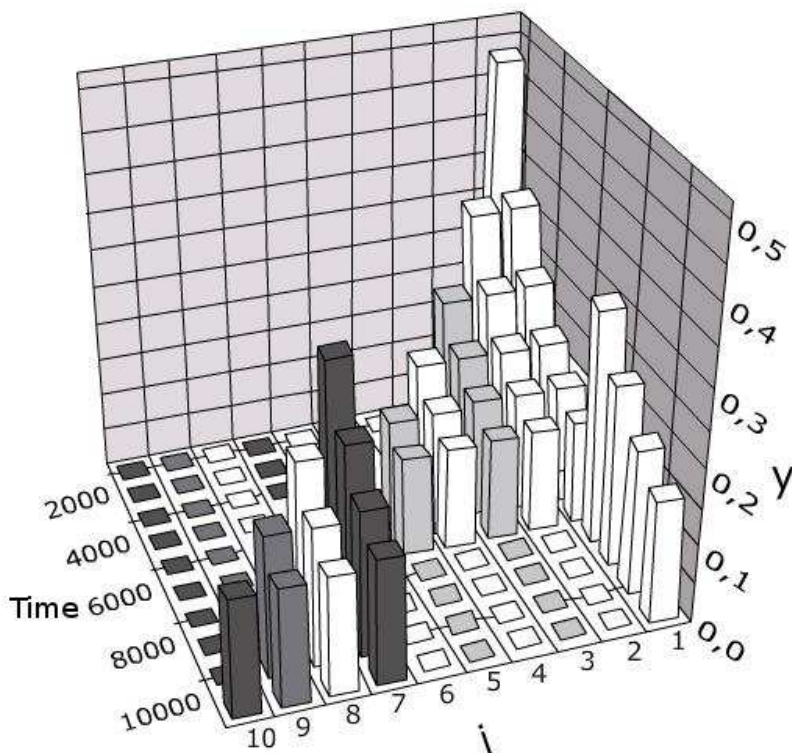


Fig. 8. Evolution of populations in memory, up to 11,000 time steps (concentration of antigens equal to 0.10 a.u.). The first and seventh clonal populations remain excited, while the others disappear - except for the last populations, which were excited near the end of the range.

This behavior occurs because the immune system has a maximum number of cells that it can support; in other words, when new antigens are memorized, others need to be forgotten (immune homeostasis turnover). At time step 7,000, when the seventh inoculation is performed, the first population begins to increase, indicating that it can be stored for a long period. In our Ag-dependent approach, this behavior indicates that an increase in the lifetime (lifespan) of memory can be generated by antigen survival (antigenic dependence).

3.2 Antigen mutation

To study the influence of antigenic mutation on memory (B cell antigen-dependent memory), simulations of inoculations of the 30 samples were also performed, with an antigenic dosage of

$Ag_{initial} = 0.1 a.u.$ The durations of memory populations in each experiment (E1, E2, and E3) are shown in Fig.9.

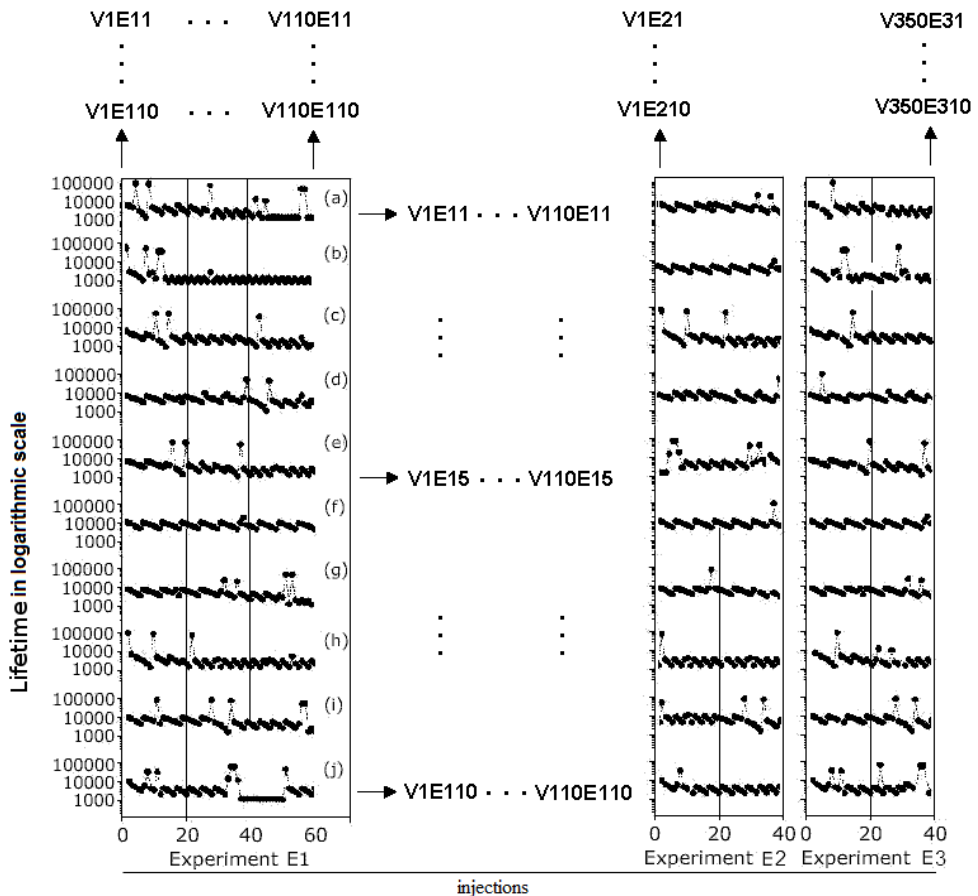


Fig. 9. Lifetime on a logarithmic scale for the clonal populations in each sample and in three experiments. For best viewing results, the graphs were truncated at 60 time steps (experiment E1) and 40 time steps (experiments E2 and E3). The arrows indicate the antigen populations that led to the production of immune memory.

In Fig. 9 (a), for example, all of the lifetimes (lasting memories) are related to antigens of different species (V1E11...V110E11). In contrast, the first lifetime in Fig. 9 (a)-(j) refers to an antigen that has already undergone mutation (V1E11...V1E110). Similar memory developments for experiments E2 and E3 are also shown in Fig. 9. The behavior of the average durability of the memories is shown in Fig. 10 (a) - (c).

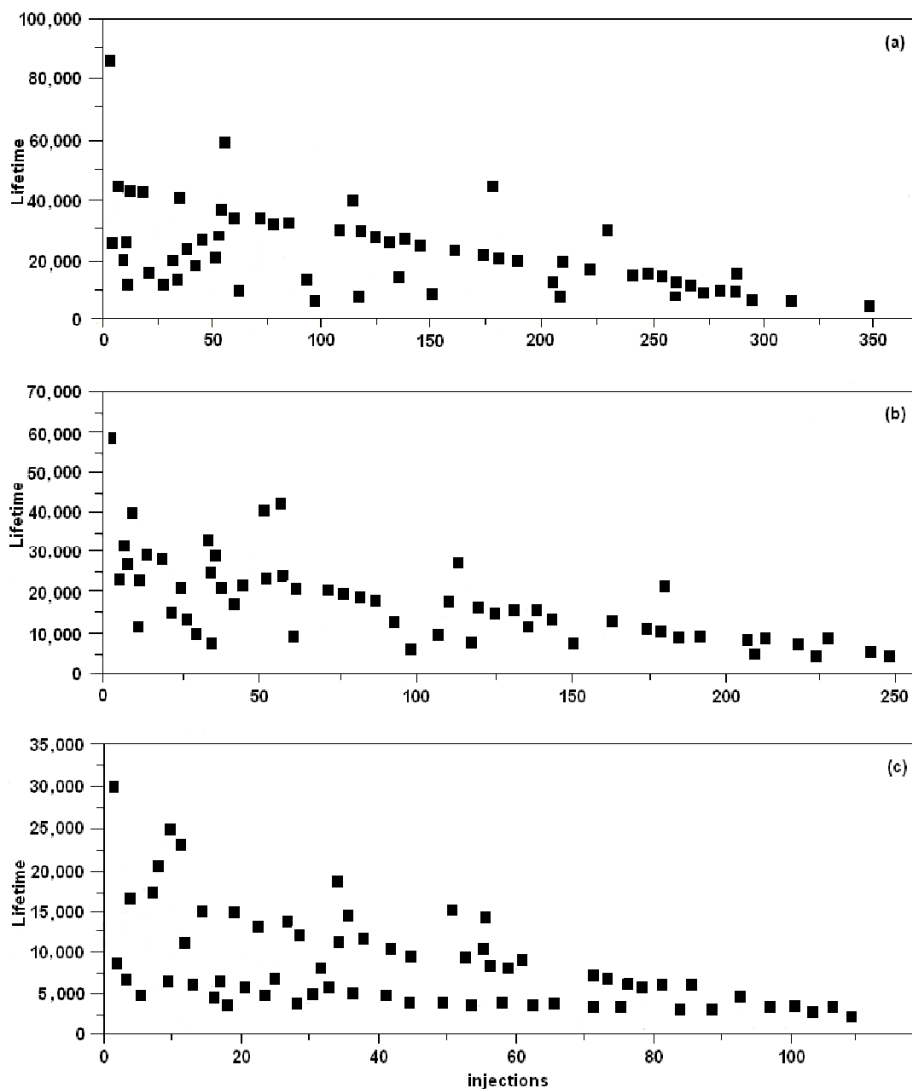


Fig. 10. Temporal averages of memory lifespans. In (a), to 350 antigen inoculations; in (b), to 250 antigen inoculations; and in (c), to 110 antigen inoculations.

The average lifespans are calculated from the memory lifespans generated by each mutated antigen, as follows:

- For experiment E1 (Fig. 10 (c)), the first average lifetime is obtained by $\frac{1}{10} \sum_{k=1}^{10} V_1 E_{1,k}$ and the last average lifetime is obtained by $\frac{1}{10} \sum_{k=1}^{10} V_{110} E_{1,k}$;

- For experiment E2 (Fig. 10 (b)), the first average lifetime is obtained by $\frac{1}{10} \sum_{k=1}^{10} V_1 E_{2,k}$ and the last average lifetime is obtained by $\frac{1}{10} \sum_{k=1}^{10} V_{250} E_{2,k}$;
- For experiment E3 (Fig. 10 (a)), the first average lifetime is obtained by $\frac{1}{10} \sum_{k=1}^{10} V_1 E_{3,k}$ and the last average lifetime is obtained by $\frac{1}{10} \sum_{k=1}^{10} V_{350} E_{3,k}$.

From Figs 9 and 10, the resulting set for this dynamics suggests that different antigens, and mutated antigens, generate different lifespans for immunological memory.

4. Discussion and conclusion

In this paper, an Ag-dependent mathematical model was used to explore how the key elements of the adaptive immune system function. The same model was also used to investigate the factors that are potentially responsible for maximum immunization capacity [40-55].

Inspired by the following statement of Elgueta et al.: "After 20 years, the role for persisting antigens, immune complexes, and FDCs is still not satisfactorily resolved [...] It is completely unknown how the memory B cell compartment is sustained [...] The role of antigens, FDCs, and immune complexes is still open to further investigation" [56], we have paid special attention to the phenomenon of immune memory and its relationship to antigen mutation and antigenic persistence.

Our results suggest that not only antigen type but also antigen mutation can influence the durability of immunizations, indicating that the role of antigen persistence is important for prolonging immune memory. These results were discussed with respect to recent work, and we refer to the adoption of parameter values chosen among data gathered from the literature. The model used in this study took into consideration that the immune system is a network of molecules and cells that can recognize itself [1-6,17]. The cells that recognize antigens select a complementary set of clones (anti-idiotypic antibodies) that can react with the idiotypes of other cells. Thus, the clonal expansion of complementary cells can also occur when these two types of cells interact through lock-and-key connections [8]. In the results presented here, such behavior was observed when an antigen was inoculated into the system and two B cell populations were excited: the population of cells that recognized the antigen and the population of cells that recognized its complementary shape, as shown in Fig. 7.

The results also show that an important factor in the durability of immunological memory is the mutation of antigen populations. In 2009, Tarlinton *et al.* [49] published a review paper, suggesting that the homeostasis of immune memory can only occur if new memory populations arise over others, i.e., to create dynamic equilibrium among memory cells, some need to disappear for others to arise, because the immune system has a maximum memory capacity [40-55]. Choo *et al.*, in a recent paper published in *The Journal of Immunology* [57], reported the same finding, based on the Ag-independent premise. Choo *et al.* (2010) have

determined, by means of a quantitative analysis, that the homeostatic turnover of Ag-specific CD8 memory T cells is stochastic rather than deterministic.

Then, the results we show in Fig. 8 indicate, in part, an alignment with the work of Choo *et al.* (2010) and with that of Tarlinton *et al.*, because some populations were "forgotten" so that others could be "memorized", thereby complying with the principle of homeostatic turnover. However, Tarlinton *et al.* (2008) [49] and Choo *et al.* (2010) [57] suggest that the mechanism for achieving homeostasis is stochastic, contrary to earlier work of Matzinger (1995)[50] and Nayak *et al.* (2001)[19], who indicated that the durability of memory depends on the antigen type.

The results presented in Figs. 9 and 10 suggest that the homeostatic turnover of a memory B cell depends on the antigen type and also on their mutation(s). Thus, our model aligns best with the earlier work of Nayak *et al.* (2001) and Matzinger *et al.* (1995), and it also aligns to some extent with the work of Tarlinton *et al.*, specifically with respect to storage capacity (homeostatic turnover). However, our results do not line up with a hypothesis of randomness (stochastically) for the kinetics of immune memory, as inferred by Choo *et al.*

The results presented here considered a pool of B cells, but similar conclusions can be drawn from a pool of CD4 T cells. In our simulations, memory lifespan is dependent on the antigen, and the dynamic behavior of memory is strongly deterministic. These results are especially interesting, because they may suggest a deterministic chaotic behavior for the immune memory. In chaotic behavior, there is a mix of stochasticity and determinism, i.e., there exists a well-defined mathematical function for the problem, but small changes in initial conditions can lead to unpredictable results. In conclusion, our results have shown that Choo *et al.* (2010) may have inferred an "apparent" stochastic behavior for homeostatic turnover in their work; however, this behavior may be linked to a deterministic-chaotic dynamic equilibrium. Nevertheless, this finding also indicates that, although the memory behavior is deterministic, just is possible to predict the durability of immunization inferred by a vaccine within a limited interval of antigenic concentration, i.e., outside chaotic region.

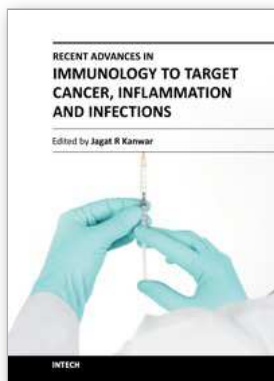
5. References

- [1] Farmer, J. D., Packard, N. H., Perelson, A. S. *The Immune System, Adaptation, and Machine Learning*. Physica D, Amsterdam, v. 22, pp. 187-204, July 1986.
- [2] Roitt, I., Brostoff, J., Male, D. *Immunology*. 4th Ed. New York: Mosby, 1998.
- [3] Hofmeyr, S. A. *An Interpretative Introduction to the Immune System Design*. In: *Principles for the Immune System and Other Distributed Autonomous Systems*. Cohen, I., Segel, L. A. (eds.). Oxford: Oxford University Press, pp. 302-340, 2000.
- [4] Klein, J. *Immunology*. Oxford: Blackwell Scientific Publications, 1990.
- [5] Lederberg, J. *Ontogeny of the Clonal Selection Theory of Antibody Formation*. *Annals of the New York Ac. of Sc.*, v. 546, pp. 175-182, 1988.
- [6] Perelson, A. S., Weisbuch, G. *Immunology for Physicists*. *Rev. of Modern Physics*, Seattle, v. 69, n. 4, pp. 1219-1267, Oct. 1997.
- [7] Celada, F., Seiden, P. *A computer model of cellular interaction in the immune system*. *Immunology Today*, Amsterdam, pp. 1356-1362, February 1992.
- [8] Perelson, A. S., Mirmirani, M., Oster, G. F. *Optimal Strategies in Immunology II. B Memory Cell Production*. *J. Math. Biol.*, Oxford, v. 5, pp. 213-256, October 1978.

- [9] Kaufman, M., Urbain, J., Thomas, R. *Towards a logical analysis of the immune response*. J. Theor. Biol., Amsterdam, v. 11, pp. 527-561, January 1985.
- [10] Kaufman, M., Weinberg, E. D. *The NK Model of Rugged Fitness Landscapes and Its Application to Maturation of the Immune Response*, J. Theor. Biol., Amsterdam, v. 141, pp. 211-245, December 1989.
- [11] Celada, F., Seiden, P. *Affinity maturation and hypermutation in a simulation of the humoral immune response*. Eur. J. Immunol., Weinheim, v. 26, pp. 1350-1358, June 1996.
- [12] Menchón, S. A., Ramos, R. A., Condat, C. A. *Modeling subspecies and the tumor-immune system interaction: Steps toward understanding therapy*. Physica A: Statistical Mechanics and its Applications, v. 386, pp. 713-719.
- [13] MO, H. *Review of Modeling and Stimulating Human Immune System. Artificial Intelligence Applications and Innovations*. IFIP International Federation for Information Processing, 2005, v. 187/2005, pp. 845-854.
- [14] Rapin, N., Lund, O., Bernaschi, M., Castiglione, F. *Computational Immunology Meets Bioinformatics: The Use of Prediction Tools for Molecular Binding in the Simulation of the Immune System*. PLoS One. v. 5(4), p. e9862, 2010.
- [15] Lundegaard, C., Lund, O., Kesmir, C., Brunak, S., Nielsen, M. *Modeling the adaptive immune system: predictions and simulations*. Bioinformatics. v. 23, pp. 3265-3275, 2007.
- [16] Boer, R. J., Oprea, M., Rustom, A., Murali-Krishna, K., Ahmed, R., Perelson, A. *Recruitment Times, Proliferation, and Apoptosis Rates during the CD8+ T-Cell Response to Lymphocytic Choriomeningitis Virus*. JOURNAL OF VIROLOGY, v. 75, pp. 10663-10669, 2001.
- [17] Jerne, N. K. *Towards a Network Theory of the Immune System*. Ann. Immunol. v. 125C, pp. 373-389, October 1974.
- [18] Shibani Mitra-Kaushik, S., Shaila, M. S., Anjali K. Karande, A. K., Nayak, R. *Idiotype and Antigen-Specific T Cell Responses in Mice on Immunization with Antigen, Antibody, and Anti-idiotypic Antibody*. Cellular Immunology v. 209, pp. 109-119, 2001.
- [19] Nayak, R., Mitra-Kaushik, S., M. S. Shaila. *Perpetuation of immunological memory: a relay hypothesis*. Immunology v. 102, pp. 387-395, 2001.
- [20] Castro, L. N. *Fundamentals of Natural Computing: Basic Concepts, Algorithms, and Applications*. Chapman & Hall/CRC Computer & Information Science Series, 2006.
- [21] Lagrecia, M. C., Almeida, R. M. C., Santos, R. M. Z. *A Dynamical Model for the Immune Repertoire*, Physica A, v. 289, pp. 191-207, 2001.
- [22] Ausloos, M., Dirickx, M. *The Logistic Map and the Route to Chaos*. 413 p. Springer, 2006.
- [23] Heyman, B. *Feedback regulation by IgG antibodies*. Immunology Letters, v. 88, pp. 157-161, 2003.
- [24] Hjelm, F., Carlsson, F., Getahun, A., Heyman, B. *Antibody-Mediated Regulation of the Immune Response*. Scandinavian Journal of Immunology, v. 64, 177-184, 2006.
- [25] Nimmerjahn, F., Ravetch, J. V. *Antibody-mediated modulation of immune responses*, v. 236, pp. 265-275, 2010.
- [26] Ferrari, P. C., Angotti, J. A. P., Tragtenberg, M. H. R. *Introdução ao Caos em Sistemas Dinâmicos*. Mini-curso. Instituto de Física – UFG, 2006.
- [27] May, R. M. *Simple Mathematical Models with Very Complicated Dynamics*. Nature, V. 261, p. 459, 1976.

- [28] Aubin, D., Dalmedico, A. D. *Writing the History of Dynamical Systems and Chaos: Longue Dureé and Revolution, Disciplines and Cultures*. *Historia Mathematica*, v. 29, pp. 273-339, 2002.
- [29] Erneux, T. *Applied delay differential equations*. In: *Surveys and Tutorials in the Applied Mathematical Sciences*. Springer, p. 210, 2009.
- [30] Moreira, I. C. *Os primórdios do Caos Determinístico*. *Ciência Hoje*, v. 14, pp. 10-16, 1992.
- [31] Dudek, M. R. *Lotka-Volterra Population Model of Genetic Evolution*. *Communications in Computational Physics*, v. 2, pp. 1174-1183, 2007.
- [32] Bagnoli, F., Bezzi, M. Eigen's Error Threshold and Mutational Meltdown in a Quasi-species Model, *International Journal of Modern Physics C*, v. 9, pp. 1-7, 1998.
- [33] Gould, H., Tobochnik, J. *An Introduction to Computer Simulation Methods: Applications to Physical Systems*. Addison-Wesley Publishing Company. 1996.
- [34] von Laer, D., Hasselmann, S., Hasselmann, K. *Impact of gene-modified T cells on HIV infection dynamics*. *Journal of Theoretical Biology*, v. 238, pp. 60-77, 2008.
- [35] Walker, R. E., Carter, C. S., Muul, L., Natarajan, V., Herpin, B. R., Leitman, S. F., Klein, H. G., Mullen, C. A., Metcalf, J. A., Baseler, M., Falloon, J., Davey, R. T., Kovacs, J. A., Polis, M. A., Masur, H., Blaese, R. M., Lane, H. C. *Peripheral expansion of pre-existing mature T cells is an important means of CD4⁺ T-cell regeneration HIV-infected adults*. *Nat. Med.* v. 4, pp. 852-856, 1998.
- [36] Heyman, B. *Regulation of Antibody Responses via Antibodies, Complements, and FC Receptors*. *Annu. Rev. Immunol.* v. 18, pp. 709-737, 2000.
- [37] Rustom Antia, r., Pilyugin, s. s., Ahmed, r. *Models of immune memory: On the role of cross-reactive stimulation, competition, and homeostasis in maintaining immune memory*. *Immunology*, v. 95, pp. 14926-14931, 1998.
- [38] Monvel, J. H. B., Martin, O. M. *Memory capacity in large idiotypic networks*. *Bulletin of Mathematical Biology*. v. 57, pp. 109-136, 1995.
- [39] Vani, J., Elluru, S., Negi, V., Lacroix-Desmazes, S., Michel D. *Role of natural antibodies in immune homeostasis: IVIg perspective*. *Autoimmunity Reviews*, v. 7, pp. 440-444, 2008.
- [40] Etchegoin, P. G. *Vaccination pattern affects immunological response*. *Physica A: Statistical Mechanics and its Applications*, v. 354, pp. 393-403, 2005.
- [41] Boer, R. J., Oprea, M., Rustom. A., Murali-Krishna, K., Ahmed, R., Perelson, A. *Recruitment Times, Proliferation, and Apoptosis Rates during the CD8⁺ T-Cell Response to Lymphocytic Choriomeningitis Virus*. *Journal of Virology*, v. 75, pp. 10663-10669, 2001.
- [42] Bueno, V., Pacheco-Silva, A. *Tolerância oral: uma nova perspectiva no tratamento de doenças autoimunes*. *Revista da Associação Médica Brasileira*, v. 45, pp. 79-85, 1999.
- [43] Lima, F. A., Carneiro-Sampaio, M. *The role of the thymus in the development of the immune system*. *Reviews and Essays*, v. 29, pp. 33-42, 2007.
- [44] Utzny, C., Burroughs, N. J. *Long-term Stability of Diverse Immunological Memory*. *J. Theor. Biol.*, v. 211, pp. 393-402, 2001.
- [45] Yao, W., Hertel, L., Wahl, L. M. *Dynamics of recurrent viral infection*. *Proc. R. Soc. B*, v. 273, pp. 2193-2199, 2006.
- [46] Dimitrijevic, L., Zvancevic-Simonovic, S., Istojanovic, M., Inic-Kanada, A., Ivkovic, I. *The Possible Role of Natural Idiotoxes in Immune Memory*. *Clinical & Developmental Immunology*, v. 11, pp. 281-285, 2004.

- [47] Obukhanych, T. V., Nussenzweig, M. C. *T-independent type II immune responses generate memory B cells*. *Journal of Experimental Medicine*, v. 203, pp. 305-310, 2006.
- [48] Lanzavecchia, A., Sallusto, F. *Human B cell memory*. *Current Opinion in Immunology*, v. 21, pp. 298-304, 2009.
- [49] Tarlinton, D., Radbruch, A., Hiepe, F., Thomas Dorner, T. *Plasma cell differentiation and survival*. *Current Opinion in Immunology*, v. 20, pp. 162-169, 2008.
- [50] Matzinger, P. *Immunology: memories are made of this?* *Nature*, pp. 369-605, 1995.
- [51] Hendrikxa, L. H., Berbersa, G. A. M., Veenhovenb, R. H., Sandersc, E.A.M., Buismana, A. M. *IgG responses after booster vaccination with different pertussis vaccines in Dutch children 4 years of age: Effect of vaccine antigen content*. *Vaccine*, v. 27, pp. 6530-6536, 2009.
- [52] Tizard, I. R. *Immunology: An Introduction*. 4th ed. Philadelphia: Saunders College Publishing, 1995.
- [53] Abbas, A. K., Lichtman, A. H., Pober, J. S. *Cellular and Molecular Immunology*.
- [54] Kamradt, T., Avrion, M. N. *Advances in immunology: Tolerance and Autoimmunity*. *N Engl J Med*, v. 344, pp. 655-64, 2001.
- [55] Peter, D., Roitt, I. M. *Advances in immunology: The Immune System*. *New Engl. J. Med.*, v. 343, pp. 37-49, 2000.
- [56] Elgueta, R., Vries, V. C., Noelle, R. J. *The immortality of humoral immunity*. *Immunological Reviews*, v. 236, pp. 139-150, 2010.
- [57] Choo, D. K., Murali-Krishna, K., Anita, R., Ahmed, R. *Homeostatic Turnover of Virus-Specific Memory CD8 T Cells Occurs Stochastically and Is Independent of CD4 T Cell Help*. *Journal of Immunology*, v.185, pp. 3436-44, 2010. Esta precisa ser a referência número 1.



Recent Advances in Immunology to Target Cancer, Inflammation and Infections

Edited by Dr. Jagat Kanwar

ISBN 978-953-51-0592-3

Hard cover, 520 pages

Publisher InTech

Published online 09, May, 2012

Published in print edition May, 2012

Immunology is the branch of biomedical sciences to study of the immune system physiology both in healthy and diseased states. Some aspects of autoimmunity draws our attention to the fact that it is not always associated with pathology. For instance, autoimmune reactions are highly useful in clearing off the excess, unwanted or aged tissues from the body. Also, generation of autoimmunity occurs after the exposure to the non-self antigen that is structurally similar to the self, aided by the stimulatory molecules like the cytokines. Thus, a narrow margin differentiates immunity from auto-immunity as already discussed. Hence, finding answers for how the physiologic immunity turns to pathologic autoimmunity always remains a question of intense interest. However, this margin could be cut down only if the physiology of the immune system is better understood. The individual chapters included in this book will cover all the possible aspects of immunology and pathologies associated with it. The authors have taken strenuous effort in elaborating the concepts that are lucid and will be of reader's interest.

How to reference

In order to correctly reference this scholarly work, feel free to copy and paste the following:

Alexandre de Castro (2012). An Ag-Dependent Approach Based on Adaptive Mechanisms for Investigating the Regulation of the Memory B Cell Reservoir, Recent Advances in Immunology to Target Cancer, Inflammation and Infections, Dr. Jagat Kanwar (Ed.), ISBN: 978-953-51-0592-3, InTech, Available from: <http://www.intechopen.com/books/recent-advances-in-immunology-to-target-cancer-inflammation-and-infections/an-ag-dependent-approach-based-on-adaptive-mechanisms-for-investigating-the-regulation-of-the-memory>

INTECH
open science | open minds

InTech Europe

University Campus STeP Ri
Slavka Krautzeka 83/A
51000 Rijeka, Croatia
Phone: +385 (51) 770 447
Fax: +385 (51) 686 166
www.intechopen.com

InTech China

Unit 405, Office Block, Hotel Equatorial Shanghai
No.65, Yan An Road (West), Shanghai, 200040, China
中国上海市延安西路65号上海国际贵都大饭店办公楼405单元
Phone: +86-21-62489820
Fax: +86-21-62489821

© 2012 The Author(s). Licensee IntechOpen. This is an open access article distributed under the terms of the [Creative Commons Attribution 3.0 License](#), which permits unrestricted use, distribution, and reproduction in any medium, provided the original work is properly cited.